Comparison Between CNN and GNN Pipelines for Analysing the Brain in Development

Antoine Bourlier[1,2], Elodie Chaillou[2], Jean-Yves Ramel[3] and Mohamed Slimane[1]
[1]*LIFAT, Université de Tours, 64 Av. Jean Portalis, Tours, France*
[2]*INRAe, CNRS, Université de Tours, Nouzilly, France*
[3]*LISTIC, Université de Savoie Mont-Blanc, Chambéry, France*

Keywords: Graph, Machine Learning, MRI, Segmentation.

Abstract: In this study, we present a new pipeline designed for the analysis and comparison of non-conventional animal brain models, such as sheep, without relying on neuroanatomical priors. This innovative approach combines an automatic MRI segmentation with graph neural networks (GNNs) to overcome the limitations of traditional methods. Conventional tools often depend on predefined anatomical atlases and are typically limited in their ability to adapt to the unique characteristics of developing brains or non-conventional animal models. By generating regions of interest directly from MR images and constructing a graph representation of the brain, our method eliminates biases associated with predefined templates. Our results show that the GNN-based pipeline is more efficient in terms of accuracy for an age prediction task (63.22%) compared to a classical CNN architecture (59.77%). GNNs offer notable advantages, including improved interpretability and the ability to model complex relational structures within brain data. Overall, our approach provides a promising solution for unbiased, adaptable, and interpretable analysis of brain MRIs, particularly for developing brains and non-conventional animal models.

1 INTRODUCTION

Automated methods have facilitated brain MRI analysis, especially in humans and conventional animal models (Kaur and Gaba, 2021; Park and Friston, 2013). However, such tools are rarely available to study developing brains or non-conventional animal models like sheep. In these cases, brain structures identification is often manual or based on automatic segmentation using signal intensity and templates, when available (Nitzsche et al., 2015; Ella et al., 2017). These methods depend on biological priors and the accuracy of atlases, which may not fully capture individual variations or patterns associated to different brain disorders. These issues are especially challenging for developing brains, where contrast is weak, development is uneven, and some structures are not visible (Li et al., 2019). Additionally, using predefined regions may limit the discovery of new brain correlates.

To address segmentation bias, convolutional neural networks (CNNs) have been introduced, as they work directly on MR images without segmentation (Srinivasan et al., 2024; Coupeau et al., 2022). CNNs provide valuable whole-brain or abnormality-level information but require large labelled datasets to learn low-level image features for classification or segmentation tasks. This makes them unsuitable for the developing brain or non-conventional animal models with small cohorts.

In this paper, we present a pipeline to address both segmentation biases and CNN limitations. We propose generating regions of interest (ROIs) without relying on neuro-anatomical priors. We use voxel intensities to create segmented images via 2 different segmentation algorithms. Additionally, we use graph neural networks (GNNs) to identify and analyse anatomical patterns, as GNNs model the brain as interconnected patches, capturing complex relationships between regions (Cui et al., 2021; Li et al., 2021; Ravinder et al., 2023). By avoiding predefined atlases, our method allows more flexible, image-driven exploration of the brain. This approach is particularly useful for studying non-conventional animal models of brain development, such as sheep. It offers the potential to discover new structures and patterns in both human and animal studies, enhancing under-

Bourlier, A., Chaillou, E., Ramel, J.-Y. and Slimane, M.
Comparison Between CNN and GNN Pipelines for Analysing the Brain in Development.
DOI: 10.5220/0013173500003912

In *Proceedings of the 20th International Joint Conference on Computer Vision, Imaging and Computer Graphics Theory and Applications (VISIGRAPP 2025) - Volume 3: VISAPP*, pages 475-482
ISBN: 978-989-758-728-3; ISSN: 2184-4321

standing and improving the diagnosis and treatment of developing brain disorders.

This paper focuses on the specific task related to study the developing brain. We tested various GNN architectures and compared them to a classical CNN approach. The comparison addresses the challenge of predicting brain age in non-conventional animal models without neuro-anatomical priors. The next sections discuss the limitations of classical brain MRI processing methods to study developing brain disorders and non-conventional animal models. We detail our pipeline, including segmentation, graph generation, and GNN prediction. Then, we present the experimental comparison with a CNN approach, followed by a discussion of its advantages and limitations.

2 RELATED WORKS

2.1 Classical Approaches Used on Brain MRI

The 2 main tasks studied in the literature are image/brain segmentation (Coupeau et al., 2022) and image/brain classification (Srinivasan et al., 2024; Kaur and Gaba, 2021; Poriya, 2023). In both cases, machine learning algorithms provide powerful tools such as CNN and graph convolutional network (GCN) layers that compute and find on its own the most relevant features. Whether CNN or GNN is chosen, both require specific key such as pre-processing and patch extraction. The aim of the MRI pre-processing (denoising, normalisation etc.) is to adjust the intensity values of the images to a standard range in order to ensure consistency. A resampling step is used to align images to a common voxel size or resolution and a registration step can be added to align images to a standard anatomical space, often using a template brain. To remove non-brain tissues (e.g., skull, scalp) cropping and skull-stripping are performed on MRI images.

2.1.1 Segmentation

The aim of segmentation is to delineate and identify anatomic ROI in the brain MRI, segmented images being used to create a graph representation. Segmentation is performed manually or using atlases based on individual brain images or templates (Van Essen and Drury, 1997; Yang et al., 2020; Fil et al., 2021). They are used for ROI identification, delineating various regions and structures or serve as reference points to align individual MRI scans to a common space, facilitating consistent and accurate analysis across subjects.

2.1.2 CNN Design

A CNN typically consists of multiple layers, including convolutional layers, pooling layers, and fully connected layers. Using advanced CNN architectures, such as AlexNet (Krizhevsky et al., 2012), or ResNet (He et al., 2016), enhances the model's ability to learn complex patterns and achieve high performance in various MRI analysis tasks, including classification, clustering etc. Incorporating biological priors through brain atlases can further refine these methods, offering improved accuracy and consistency in brain MRI analysis. Concerning brain age prediction, several CNN architectures have been proposed including VGG, ResNet, and DenseNet (Cole et al., 2017; Jiang et al., 2020).. More advanced CNN architectures including attention mechanisms have since been developed to boost the representational power and improve prediction accuracy (Lam et al., 2020; Cheng et al., 2021).

2.1.3 Graph Design

Nodes of a graph are usually defined at a region level (i.e., one node per brain structure). The way the regions are chosen is really linked with the aim of the study and could represent neurons, anatomical structures, brain tissues, voxels, etc. From an anatomical point of view, node features provide information about the position of the region (coordinates of the center of gravity, orientation etc.), the shape (volume, sphericity etc.), the signal intensity, which is useful to understand the composition of the tissue, etc. Graph theory features can also be used (centrality, strength etc.). Several ways exist to build the edges of the graph and characterise them depending on the aim of the study. Generally, three types of edges are distinguished: structural, functional, and effective connections (Fedorov et al., 2012). The possibilities for edge features are also numerous: Euclidean distances, tract lengths, connection costs, etc. (Bullmore and Bassett, 2011; Sporns, 2018). Possibly, the trickiest component in creating the brain network lies in edge creation. We could create a fully connected graph but for an interpretable and efficient representation, we aim to reduce the edge density, so that only the significant connections are displayed. This is achieved by introducing a threshold and removing edges that do not meet the required criteria. How to define the threshold is still an active research question: typical approaches use customised, statistical, or expert-based criteria.

2.1.4 GNN Design

Once the brain has been modelled as a graph, GNNs are trained to analyse these graphs, and to capture complex relationships and variations in brain organisation (Li et al., 2021; Ravinder et al., 2023; Srinivasan et al., 2024; Coupeau et al., 2022). For age prediction, GNN architectures have also been proposed to better exploit the inter-region relationships like a GNN architecture that processes diffusion-MRI-derived brain connectivity data while considering brain network topological locality (Sporns, 2007). Many methods like multi-hop graph attention or graph Transformer framework require graph structures such as tractography networks or the registration of multi-modal images based on a standard brain template (Lim et al., 2024; Cai et al., 2023).

2.2 Approaches for Brain in Development and Non-Conventional Animal Model

The analysis of brains in development and/or from non-conventional animal models, rises several challenges and considerations that differ from the analysis of adult human brains. The primary differences include anatomical variations, the lack of standardised atlases, tools and often smaller datasets.
For example, brain segmentation of non-conventional animal models is often done manually. This process is time-consuming, requires neuro-anatomical expertise and introduces a high level of bias due to inter-individual variation between operators (Fedorov et al., 2012). An alternative to the manual segmentation, is the atlas-based registration method. The concept involves creating a template, achieved by registering and normalising multiple brain MR images into a common space using affine transformations, followed by segmentation of the template and transferring the segmentation to each MR image (De Vico Fallani et al., 2017). While this method is beneficial for segmenting numerous images simultaneously, post-processing is essential to ensure accurate correspondence between the segmentation and individual anatomy.
There are also some automatic and incremental segmentation algorithms available that incorporate biological priors (Galisot et al., 2022).

3 THE PROPOSED PIPELINE

3.1 From 3D MR Images to Graphs

We propose a generic pipeline for transforming 3D MR images of brains in development of non-conventional animal models into graphs. The objective is to generate graphs incorporating a maximum of information from the brains and, to let the GNN select the useful information inside these graphs (Figure 1).

3.2 Pre-Processing

Pre-processing includes skull-stripping and z-score normalisation. Z-score normalisation is reported to be more suitable for brain MRI analysis, particularly in machine learning, because it maintains the alignment of intensity peaks for white matter, grey matter, and CSF (Schmid, 2023). After the image pre-processing, the graph creation is divided into two parts: node creation and edge creation.

3.3 Nodes and Edges Creation

The creation of nodes corresponds to segmented ROIs (Figure 2). Since our goal is to process brains in development of growing non-conventional animal models, segmentation without biological priors offers an alternative approach to analyse brain MR images and constructing graphs. This method relies solely on image information and the data is treated purely as a conventional image rather than specifically as a brain image. For this study, we have chosen to test a histogram-based clustering algorithm and a "split and merge" algorithm. The histogram-based algorithm splits the intensity range into N equal parts. One of the main challenges is to determine the optimal parameters of the algorithm which depends on the study objectives, the desired level of details etc. In the image 1, the first segmentation is made with this algorithm. The second algorithm is the "split and merge" algorithm, (Gonzalez and Woods, 2017) which operates in two distinct phases: "split" and "merge". In the first phase, the algorithm recursively divides the image into smaller and homogeneous regions ("cubes") based on a user-defined homogeneity criterion and a minimum region size. The homogeneity criterion is the intensity amplitude of the region intensities. Then, in the merge step, adjacent regions are combined if their merged region meets another homogeneity criterion. Each region of the segmentation is represented as a node with associated normalised features : region's volume divided by the brain's volume, region's surface area divided by the brain's surface area, mean

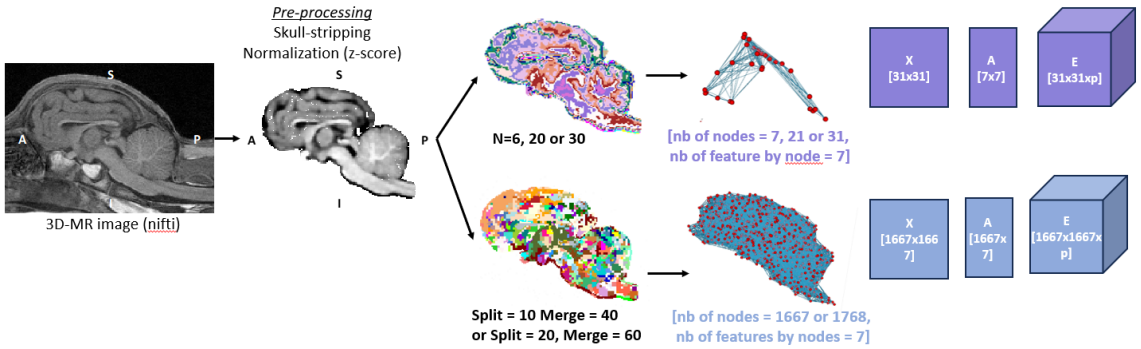

Figure 1: Graph construction pipeline in which we tested different segmentation algorithms (histogram-based segmentation and "Split and merge" segmentation) and parameters. "N" is the hyperparameter of the histogram-based algorithm. "Split" and "merge" are the hyperparameters of the "split and merge" algorithm. "p" is the number of edge features, 0 in our experiment.

intensity of the voxels inside the region, standard deviation of the intensity, region's center of gravity in the spherical coordinate system (radial distance from the center of gravity of the brain, polar angle and azimuthal angle).

Then, there are many possibilities to define the edges, and we propose to build an adjacency graph by connecting two nodes if the geometric distance between them is below a threshold d (d is a hyperparameter of the method). Depending on the task the user wants to perform with the graphs, choosing the appropriate value for d might be another challenge.

3.4 Graph Analysis and Classification

As discussed before, GNNs are particularly well-suited for brain MRI analysis due to their ability to capture the intricate relationships between different brain ROIs. Unlike CNNs, which primarily focus on local voxel information, GNNs can model the brain at a higher level where nodes represent different structures or parts of structures and edges represent connections between them. This relational representation can lead to more accurate and interpretable predictions.

In the conducted experiments, the proposed GNN architecture tries to harness these advantages to predict the age of a sheep brain (by solving a graph classification task with K classes of age range) (Figure 2).

3.4.1 Graph Convolution Layers

To propagate the information over the graph, we use a set of 3 convolution layers. As described in the previous sections, multiple convolution layers are available. Our dataset is relatively small, consisting of approximately 200 graphs. Consequently, using a complex neural network with sophisticated and large layers is not advisable. Therefore, in this study, we utilised the GCNConv layer, which considers both the node feature (F) and adjacency (A) matrices. The GCNConv layer computes updated node features by aggregating information from neighbour nodes and their connections. The input to the first layer consists of the node features matrix (F), initialized with 7 features per node, and the adjacency matrix (A) that encodes the graph structure. The transformation from 7 features to 32 or 64 features occurs progressively across the layers, as follows:

- First set of parameters: The model begins by transforming the 7 initial features into 8 features using the first GCNConv layer (Figure 2). This output is then passed to a second GCNConv layer, which further transforms it to 16 features. Finally, a third GCNConv layer transforms the features to 32 dimensions. Each layer applies a learned linear transformation followed by an activation function (ReLU in our case), enabling the network to progressively capture complex patterns in the data.
- Second set of parameters: Instead of incremental changes, the model starts with 7 features and doubles the number of dimensions at each layer: from 7 to 16, then to 32, and finally to 64. This more aggressive dimensionality increase aims to test the model's ability to learn richer representations.

Dropout regularisation is applied and set to 0.5 to prevent overfitting during training.

3.4.2 Pooling and Fully Connected Layers

A global mean pooling and a global max pooling were tested to capture interesting information while taking into account the small amount of data.

The pooled features are then passed through three fully connected (FC) layers (fc1, fc2 and fc3) to perform the classification. The first FC layer maps the features to a 128-dimensional space, the second FC

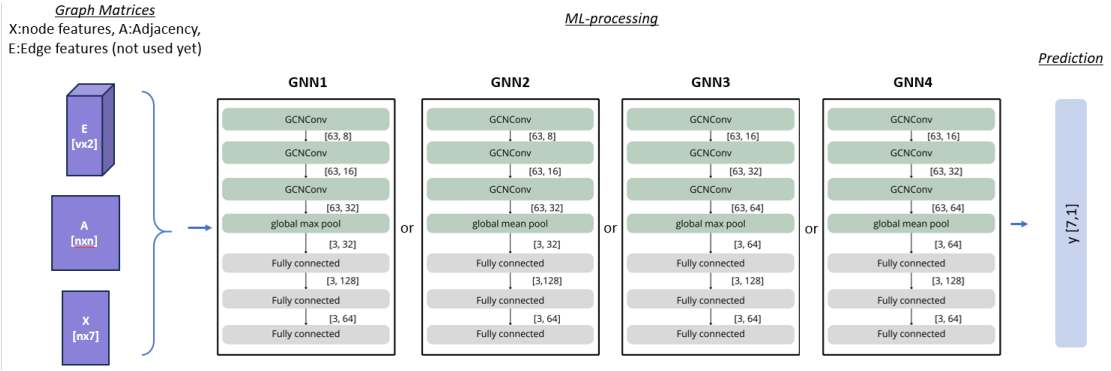

Figure 2: different GNN architectures according to the number of convolutions and the type of readout pooling have been evaluated for the different types of generated graphs presented in Figure 1.

layer to a 64-dimensional space and the third FC layer reduces this to a 7-dimensional space, to match with the (K)=7 age classes of the sheep brain.

In total, we have tested 4 different architectures by combining the 2 sets of convolution parameters and the 2 global poolings (GNN1, GNN2, GNN3 and GNN4, (Figure 2)).

4 EXPERIMENTS AND RESULTS

We conducted experiments with different CNN and GNN architectures to analyse which ones are the best suited to predict the age of brains of non-conventional animal models such as sheep. The experiments were conducted on a machine equipped with an Intel Core i7-11850H CPU running at 2.50 GHz, 32 GB of RAM, and an NVIDIA GeForce RTX A3000 Laptop GPU. All computations were performed using Python 3.11.8 with Pytorch 2.2.2+cu121 frameworks. This section describes the used datasets and protocols.

4.1 Datasets, Protocol and Metric Description

4.1.1 Datasets

The dataset used is composed of 195 3D-T1w-MRI from different projects which were all conduct in "Ile de France" growing and adult sheep from the "Unité Expérimentale de Physiologie Animale de l'Orfrasière" (UEPAO, INRAE Val de Loire, France; https://doi.org/10.15454/1.5573896321728955E12). MRI were acquired in vivo with a 3 Teslas Siemens Magnetom Verio® scanner (Erlangen, Germany) located at the imaging platform PIXANIM. A 4-channel Siemens FLEX coil was used. T1-weighted images were acquired with the 3D-MPRAGE sequence with 2 or 4 numbers of excitations according to the project. The plane resolution of the T1-w MRI was between 0.4x0.4mm and 0.5x0.5mm. We created 5 segmentations for each MRI in total : 3 from our histogram-based algorithm and 2 from our split and merge algorithm. The parameter of histogram-based algorithm is set to N=6, N=20 and N=30. N=6 gives a segmentation similar to a tissue segmentation (White matter, gray matter and CSF). The other parameters produced visually interesting results, maximizing the expressiveness of the image content while ensuring that the segmentation remains clear and not overly noisy. After testing different set of parameters we chose 2 sets of parameters for the split and merge : {homogeneity_during_split=10, homogeneity_during_merge=40, minimal_cube_size=1} and {homogeneity_during_split=20, homogeneity_during_merge=60, minimal_cube_size=1}. Each segmentation are then transformed into an adjacency graph (distance threshold d=0) with every attribute described previously.

4.1.2 Protocol and Metrics

During our experiments, we try to learn and predict the age of the subjects. Age prediction can be a hard task regarding our data. That's why we decided to learn a classification task instead of a regression task, the latter considered as more difficult to perform. We decided to distribute the images into K=7 classes of ages (Table 1) in order to obtain balanced with enough representative images into each class. The ranges associated with each class have been defined based on available data, corresponding to 10 to 20 days (with no data available for the range between 70 to 120 days).

The proposed pipelines based on GNN architectures were compared with a classical CNN architecture working with low level image features (Figure 3). In the following we compare our pipeline with the CNN architecture that presented the best results after

Table 1: Organization of the 7 classes according to the range of age (days) and number of subjects per class.

Class	1	2	3	4	5	6	7
Age (days)	0-10	11-20	21-30	31-40	41-50	51-70	123-139
Numbers	33	16	22	24	61	24	15

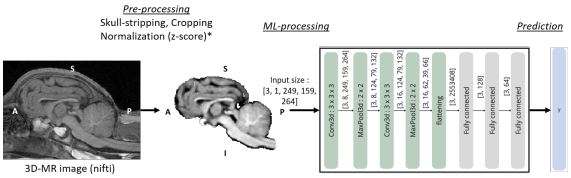

Figure 3: Optimized CCN pipeline. The architecture contains 2 convolution layers (Conv3d), a flattening layer and 3 linear layers.

learning with different layer numbers and sizes. The CNN consists of a 3D convolution layer with a kernel size of 3x3x3, followed by a 3D max-pooling layer of size 2x2. This sequence of convolution and pooling layers is repeated once. The output is then flattened into a vector, which is passed through three fully connected layers that progressively reduce its size to 128, 64, and finally 7 dimensions.

The 195 images (see dataset section) were used to create the training (50% of the MR-images), the validation (25% of the MR-images) and the test datasets (25% of the MR-images). We carefully design the test dataset to be representative of all the data by balancing the classes and projects to remove any project bias. We performed a shuffle split validation which is well suited for small datasets. The training lasts 300 epochs. The loss function is the cross-entropy loss with a learning rate of 0.001.

4.2 Results

In terms of accuracy, the GNN pipeline remains better than a classical CNN pipeline with an average accuracy of 63.22% compared to 59.77% for the CNN (table 2). These results show that our pipeline could be convenient for a classical task like age prediction. The split and merge pipelines seem to perform better than the histogram-based pipelines achieving an average accuracy of 51.43% compared to 37.73%. This could be explained by the fact that the number of nodes is not fixed and could be discriminative between the classes. For example, we found that class 6 has an average of 1,110 nodes, compared to 2,205 for class 7, making it very easy to discriminate between them.

Concerning the GNN architecture, the GNN with global better results was the GNN4 with a conv1=16, conv2=32, conv3=64 and a global mean pooling with an average accuracy of 45.08%. The other architectures have the following average accuracies : GNN1 = 43.49%, GNN2 = 40.48% and GNN3 = 43.81%. These results suggest that the global max pooling is a little bit better in average. Other pooling methods and architectures need to be experimented.

We calculated the confusion matrix of each training and the table 3 is one of them. The mean accuracy of the 3 trainings is 63.22% and this matrix is one of the 3 trainings and has a score of 63.79% of accuracy. The rows denote the true classes and the columns are the predicted classes. The results described in this confusion matrix are quite representative of this GNN model and graph creation method (which is the best configuration). We can see that 86.2% of the predictions are either correct or off by only one age class.

5 CONCLUSION AND PERSPECTIVES

In this study, we propose a novel pipeline to predict the brain age of nonconventional animal models without relying on neuro-anatomical priors to not bias the analysis. We provide an open access generic graph generation tool from 3D images available at this URL: https://scm.univ-tours.fr/projetspublics/lifat/3dbrainminer. Our proposed GNN pipeline provides better results in terms of accuracy than a traditional CNN pipeline. The process starts with automatic MRI segmentation, followed by graph transformation and analysed using a GNN model. We compared 2 segmentation algorithms with different parameters and GNN architectures.

The uniqueness of our pipeline lies in its ability to work without anatomical priors, enabling an unbiased analysis of morphofunctional features. It would be very interesting to try other parameters and especially for the split and merge algorithm, which showed promising results. Adjusting the homogeneity criterion may reveal different brain information. Improving graph transformation, particularly edge creation, could enhance learning. Using a higher distance threshold or other strategies might improve message passing in the GNN. One approach is to create all possible edges and let the GNN decide which are important during training. Edge features, not used in this study, could also provide valuable insights, such as

Table 2: Classification performances of the proposed pipelines using different segmentation methods and GNN architectures. Results are averages (with standard deviation) of performance measured over 3 shuffle splits validation. Layers and sizes of each GNN architecture : {GNN1 : conv1 = 8, conv2 = 16, conv3 = 32, maxpool; GNN2 : conv1 = 8, conv2 = 16, conv3 = 32, meanpool; GNN4 : conv1 = 16, conv2 = 32, conv3 = 64, maxpool; GNN4 : conv1 = 16, conv2 = 32, conv3 = 64, meanpool;}.

	GNN architecture	Accuracy	Recall	Precision	F1
Histogram-based n = 6	GNN1	36.78 ± 4.34	0.34 ± 0.03	0.32 ± 0.03	0.33 ± 0.03
	GNN2	35.63 ± 8.68	0.35 ± 0.05	0.32 ± 0.06	0.33 ± 0.05
	GNN3	43.10 ± 8.62	0.37 ± 0.06	0.35 ± 0.02	0.37 ± 0.04
	GNN4	41.95 ± 1.99	0.37 ± 0.03	0.38 ± 0.02	0.37 ± 0.01
Histogram-based n = 20	GNN1	31.61 ± 4.34	0.33 ± 0.06	0.31 ± 0.03	0.32 ± 0.04
	GNN2	33.33 ± 8.84	9.78 ± 16.32	0.30 ± 0.07	0.32 ± 0.08
	GNN3	30.46 ± 2.63	0.30 ± 0.01	0.29 ± 0.03	0.29 ± 0.01
	GNN4	37.92 ± 3.47	0.39 ± 0.04	0.35 ± 0.06	0.35 ± 0.04
Histogram-based n = 30	GNN1	40.81 ± 7.78	0.42 ± 0.07	0.41 ± 0.08	0.42 ± 0.08
	GNN2	37.36 ± 6.97	0.38 ± 0.07	0.35 ± 0.03	0.37 ± 0.03
	GNN3	43.10 ± 6.90	0.47 ± 0.03	0.43 ± 0.04	0.42 ± 0.05
	GNN4	40.81 ± 6.53	0.38 ± 0.08	0.39 ± 0.07	0.39 ± 0.08
Split and merge Split homogeneity = 10 Merge homogeneity = 40	GNN1	59.20 ± 8.15	0.60 ± 0.08	0.59 ± 0.10	0.59 ± 0.09
	GNN2	48.28 ± 2.98	0.53 ± 0.05	0.53 ± 0.04	0.53 ± 0.04
	GNN3	54.60 ± 7.18	0.57 ± 0.08	0.60 ± 0.11	0.58 ± 0.10
	GNN4	**63.22 ± 5.27**	0.62 ± 0.03	0.65 ± 0.07	0.62 ± 0.05
Split and merge Split homogeneity = 20 Merge homogeneity = 60	GNN1	49.05 ± 5.00	0.50 ± 0.04	0.51 ± 0.05	0.51 ± 0.04
	GNN2	47.80 ± 4.36	0.49 ± 0.09	0.53 ± 0.11	0.51 ± 0.10
	GNN3	47.80 ± 2.88	0.54 ± 0.06	0.53 ± 0.06	0.54 ± 0.06
	GNN4	41.51 ± 5.33	0.43 ± 0.08	0.48 ± 0.04	0.42 ± 0.07

Table 3: Confusion matrix of the first "shuffle split" training of the best configuration which has a score of 63.79% of accuracy.

	Predicted classes							Prediction rate
True classes	**6**	1	2	1	0	0	0	6/10
	1	**3**	0	0	0	0	0	**3/4**
	0	0	**3**	2	1	0	0	3/6
	0	0	1	**4**	1	0	0	4/6
	0	0	2	2	**12**	3	0	12/19
	0	0	1	1	2	**4**	0	4/8
	0	0	0	0	0	0	**5**	**5/5**

distances and surface contact areas.

Future research will focus on exploring various configurations and architectures to optimize our approach. More complex models, like NNConv or graph attention layers, could be incorporated to better utilize edge features. This approach enhances interpretability, often lacking in CNN methods, and offers flexibility in selecting scales or conducting multi-scale analyses for deeper insights into data structures. GNNs capture complex relationships, leading to more robust models, making them superior for tasks requiring an understanding of element relationships. Thus, we believe automatic segmentation for graph building and GNN analysis is a promising solution.

ACKNOWLEDGEMENTS

We thank Scott Love for scientific and enthusiastic discussions on brain MRI segmentations. We acknowledge the financial support the Institut National de Recherche pour l'Agriculture, l'Alimentation et l'Environnement Département Physiologie Animale (INRAE-PHASE) et Systèmes d'Élevage and the Région Centre Val de Loire for the PhD grant for Antoine Bourlier. The MR-images were acquired in projects supported by INRAE - PHASE (Neuroimagery, PhenoMatHyp, Prebiostress) and by Val de Loire regional council (Ovin2A, Convention 2013 00083140, coordinator R. Nowak, France; Neuro2Co, Convention 2017 00117257, coordinator E. Chaillou, France). This research was funded, in whole or in part, by the French National Research Agency (ANR) under the project "ANR-23-SSAI-0008-01." In line with the objective of open-access publication, the author holder applies an open-access CC-BY license to any accepted article (AAM) resulting from this submission.

REFERENCES

Bullmore, E. T. and Bassett, D. S. (2011). Brain graphs: Graphical models of the human brain connectome. 7:113–140.

Cai, H., Gao, Y., and Liu, M. (2023). Graph Transformer Geometric Learning of Brain Networks Using Multimodal MR Images for Brain Age Estimation. 42(2):456–466.

Cheng, J., Liu, Z., Guan, H., Wu, Z., Zhu, H., Jiang, J., Wen, W., Tao, D., and Liu, T. (2021). Brain Age Estimation From MRI Using Cascade Networks With Ranking Loss. 40(12):3400–3412.

Cole, J. H., Poudel, R. P. K., Tsagkrasoulis, D., Caan, M. W. A., Steves, C., Spector, T. D., and Montana, G. (2017). Predicting brain age with deep learning from raw imaging data results in a reliable and heritable biomarker. 163:115–124.

Coupeau, P., Fasquel, J. B., Mazerand, E., Menei, P., Montero-Menei, C. N., and Dinomais, M. (2022). Patch-based 3D U-Net and transfer learning for longitudinal piglet brain segmentation on MRI. 214:106563.

Cui, H., Dai, W., Zhu, Y., Li, X., He, L., and Yang, C. (2021). BrainNNExplainer: An Interpretable Graph Neural Network Framework for Brain Network based Disease Analysis.

De Vico Fallani, F., Latora, V., and Chavez, M. (2017). A Topological Criterion for Filtering Information in Complex Brain Networks. 13(1):e1005305.

Ella, A., Delgadillo, J. A., Chemineau, P., and Keller, M. (2017). Computation of a high-resolution MRI 3D stereotaxic atlas of the sheep brain. 525(3):676–692.

Fedorov, A., Beichel, R., Kalpathy-Cramer, J., Finet, J., Fillion-Robin, J.-C., Pujol, S., Bauer, C., Jennings, D., Fennessy, F., Sonka, M., Buatti, J., Aylward, S., Miller, J. V., Pieper, S., and Kikinis, R. (2012). 3D Slicer as an Image Computing Platform for the Quantitative Imaging Network. 30(9):1323–1341.

Fil, J. E., Joung, S., Zimmerman, B. J., Sutton, B. P., and Dilger, R. N. (2021). High-resolution magnetic resonance imaging-based atlases for the young and adolescent domesticated pig (*Sus scrofa*). 354:109107.

Galisot, G., Ramel, J.-Y., Brouard, T., Chaillou, E., and Serres, B. (2022). Visual and structural feature combination in an interactive machine learning system for medical image segmentation. 8:100294.

Gonzalez, R. C. and Woods, R. E. (2017). *Digital Image Processing*. Pearson, fourth edition, global edition edition.

He, K., Zhang, X., Ren, S., and Sun, J. (2016). Deep Residual Learning for Image Recognition. In *2016 IEEE Conference on Computer Vision and Pattern Recognition (CVPR)*, pages 770–778.

Jiang, H., Lu, N., Chen, K., Yao, L., Li, K., Zhang, J., and Guo, X. (2020). Predicting Brain Age of Healthy Adults Based on Structural MRI Parcellation Using Convolutional Neural Networks. 10.

Kaur, P. and Gaba, G. S. (2021). Computational Neuroscience Models and Tools: A Review. In Bhoi, A. K., Mallick, P. K., Liu, C.-M., and Balas, V. E., editors, *Bio-Inspired Neurocomputing*, Studies in Computational Intelligence, pages 403–417. Springer.

Krizhevsky, A., Sutskever, I., and Hinton, G. E. (2012). ImageNet Classification with Deep Convolutional Neural Networks. In *Advances in Neural Information Processing Systems*, volume 25. Curran Associates, Inc.

Lam, P., Zhu, A. H., Gari, I. B., Jahanshad, N., and Thompson, P. M. (2020). 3D Grid-Attention Networks for Interpretable Age and Alzheimer's Disease Prediction from Structural MRI.

Li, G., Wang, L., Yap, P.-T., Wang, F., Wu, Z., Meng, Y., Dong, P., Kim, J., Shi, F., Rekik, I., Lin, W., and Shen, D. (2019). Computational neuroanatomy of baby brains: A review. 185:906–925.

Li, X., Zhou, Y., Dvornek, N., Zhang, M., Gao, S., Zhuang, J., Scheinost, D., Staib, L. H., Ventola, P., and Duncan, J. S. (2021). BrainGNN: Interpretable Brain Graph Neural Network for fMRI Analysis. 74:102233.

Lim, H., Joo, Y., Ha, E., Song, Y., Yoon, S., and Shin, T. (2024). Brain Age Prediction Using Multi-Hop Graph Attention Combined with Convolutional Neural Network. 11(3):265.

Nitzsche, B., Frey, S., Collins, L. D., Seeger, J., Lobsien, D., Dreyer, A., Kirsten, H., Stoffel, M. H., Fonov, V. S., and Boltze, J. (2015). A stereotaxic, population-averaged T1w ovine brain atlas including cerebral morphology and tissue volumes. 9.

Park, H.-J. and Friston, K. (2013). Structural and Functional Brain Networks: From Connections to Cognition. 342(6158):1238411.

Poriya, V. (2023). Brain Tumor Classification And Segmentation Using Machine Learning For Magnetic Resonance Images.

Ravinder, M., Saluja, G., Allabun, S., Alqahtani, M. S., Abbas, M., Othman, M., and Soufiene, B. O. (2023). Enhanced brain tumor classification using graph convolutional neural network architecture. 13(1):14938.

Schmid, S. (2023). Image Intensity Normalization in Medical Imaging.

Sporns, O. (2007). Brain connectivity. 2(10):4695.

Sporns, O. (2018). Graph theory methods: Applications in brain networks. 20(2):111–121.

Srinivasan, S., Francis, D., Mathivanan, S. K., Rajadurai, H., Shivahare, B. D., and Shah, M. A. (2024). A hybrid deep CNN model for brain tumor image multi-classification. 24(1):21.

Van Essen, D. C. and Drury, H. A. (1997). Structural and Functional Analyses of Human Cerebral Cortex Using a Surface-Based Atlas. 17(18):7079–7102.

Yang, G., Zhou, S., Bozek, J., Dong, H.-M., Han, M., Zuo, X.-N., Liu, H., and Gao, J.-H. (2020). Sample sizes and population differences in brain template construction. 206:116318.